

Outer-sphere electron-transfer between horse heart cytochrome *c* and anionic Cu(II/I) complexes. Evidence for precursor formation and coordination sphere reorganization for electron transfer

Manuela Körner,^{†a} Peter A. Tregloan^b and Rudi van Eldik^{*a}

^a *Institute for Inorganic Chemistry, University of Erlangen-Nürnberg, Egerlandstr. 1, 91058 Erlangen, Germany*

^b *School of Chemistry, The University of Melbourne, Parkville, Australia 3052*

Received 12th February 2003, Accepted 11th April 2003

First published as an Advance Article on the web 2nd May 2003

The outer-sphere electron-transfer reaction between anionic bis(5,6-bis(4-sulfonatophenyl)-3-(2-pyridyl)-1,2,4-triazine)Cu(II) and cytochrome *c*^{II} was investigated as a function of pH, ionic strength, concentration, temperature and pressure. The plot of the observed pseudo-first-order rate constant as a function of the Cu(II) complex concentration showed saturation at higher Cu(II) concentrations, from which the precursor formation constant and the electron transfer rate constant could be separated ($K = (7.7 \pm 0.5) \times 10^3 \text{ M}^{-1}$ and $k_{\text{ET}} = 6.2 \pm 0.4 \text{ s}^{-1}$ at $I = 0.2 \text{ M}$, pH 7.4 and 288 K). The pseudo-first-order electron-transfer rate constant was measured as a function of temperature and pressure at (low and) high Cu(II) concentrations ($\Delta H^\ddagger = (85 \pm 4) 89 \pm 4 \text{ kJ mol}^{-1}$; $\Delta S^\ddagger = (-61 \pm 13) - 79 \pm 15 \text{ J K}^{-1} \text{ mol}^{-1}$; $\Delta G^\ddagger(288 \text{ K}) = (67.6) 66.1 \text{ kJ mol}^{-1}$; $\Delta V^\ddagger = (+8.8 \pm 0.6) + 8.0 \pm 0.7 \text{ cm}^3 \text{ mol}^{-1}$). Within the volume change for the overall reaction, the volume profile for the electron transfer step is almost symmetrical. The redox process and the change in coordination of the copper centre are proposed to be clearly separated. The back reaction between the Cu(I) complex and cytochrome *c*^{III} was investigated as a function of Cu(I) concentration at pH 7.4 at 1 bar. The observed pseudo-first-order rate constant reaches a saturation at high Cu(I) concentrations from which the precursor formation constant and the electron-transfer rate constant were estimated ($K' = (2.0 \pm 0.2) \times 10^3 \text{ M}^{-1}$ and $k'_{\text{ET}} = 0.014 \pm 0.001 \text{ s}^{-1}$ at $I = 0.2 \text{ M}$, pH 7.4 and 288 K). Simulations of the measured cyclovoltammograms applying an EC mechanism with two redox systems and two homogeneous chemical reactions were performed. The results are discussed with reference to earlier studies involving Co, Ru and Cr complexes as redox partners for cytochrome *c*.

Introduction

Redox reactions in respiratory and photosynthetic electron-transport chains are of interest from both the biological and mechanistic points of view. Many attempts have been made to define the factors that control the high selectivity of redox active enzymes towards certain substrates. The distance between and orientation of donor and acceptor molecules, the protein structure in the electron-transfer pathway, structural rearrangements coupled to the electrontransfer process, and the thermodynamic driving force may all be important.¹⁻⁸ The oxidoreductase used in this study, cytochrome *c*, takes part in the mitochondrial respiratory chain and transfers electrons from cytochrome *c*₁ to cytochrome *c* oxidase. Its three-dimensional structure is known in detail.⁹ The solvent-exposed heme edge is surrounded by lysine residues and this positively charged, basic patch is considered to be the only surface site for electron transfer to and from the heme group.^{10,11}

Biological electron transfer reactions differ from most redox processes involving small molecules. They occur rapidly over long distances (>10 Å) and are often accompanied by only small changes at the active site. In different approaches to the study of long-range electron-transfer reactions in cytochrome systems, electron-transfer reaction centers have been fixed either covalently at specific distances or electrostatically by way of association between cytochrome and the redox partner.¹²⁻¹⁵ Cytochrome *c* typically undergoes an outer-sphere electron-transfer process with metal complexes such as [Co(phen)₃]^{2+/3+}, [Co(terpy)₂]^{2+/3+} or [Ru(NH₃)₅(py)]^{2+/3+} (phen = 1,10-phenanthroline; terpy = 2,2':6',2''-terpyridine). Studies on electron-transfer reactions of metal complexes such as [Fe^{II}(EDTA)]²⁻, [Fe^{II}(CN)₆]⁴⁻ and [Co(phen)₃]^{2+/3+} with cytochrome *c* derivatives, which were singly substituted at different lysines, have led

to the construction of reactivity contour maps.¹⁶⁻¹⁸ Extended systems such as porphyrins and proteins^{11,12,19,20} require a quite precise orientation to cytochrome *c* and the reactants are most effective when the complementary charges fit the cytochrome surface structure well.

In earlier work,²¹⁻²³ we have studied the outer-sphere electron transfer reactions between cytochrome *c* and a series of complexes of the type [Ru(NH₃)₅X]^{2+/3+} (X = ammonia, pyridine, 4-ethylpyridine, isonicotinamide and 3,5-lutidine), and Co(II/III) diimine complexes. In these systems, precursor-formation was so weak that the precursor-formation constant, K , and the electron-transfer rate constant, k_{ET} , could not be separated kinetically. However, the driving force of these reactions was low enough that the kinetics of these redox reactions could be studied in both directions. This enabled us to construct volume profiles from high pressure kinetic and thermodynamic measurements for the reversible electron transfer processes. The volume profiles were found to be highly symmetrical, with the transition state located halfway between the reactant and product states. The overall volume changes seem to be mainly due to intrinsic and solvational volume changes of the redox partner of cytochrome *c*, since cytochrome *c* itself undergoes almost no volume change during the redox process.²⁴

The recently investigated, irreversible outer-sphere electron-transfer between an anionic oxochromate(V) complex and cytochrome *c*^{II} showed a clear trend towards rate saturation at high Cr(V) concentrations.²⁵ The precursor-formation constant and electron-transfer rate constant could be separated kinetically, although only under ambient pressure conditions. The volume profile constructed for that electron-transfer process, based on the effect of pressure on the overall second-order rate constant, revealed a non-symmetrical location of the transition state. It was concluded that the process is characterized by a "late" (product-like) transition state. This could be accounted for in terms of the effective precursor-complex formation found for

that system, in contrast to the apparent absence of such precursor formation in the case of the ruthenium and cobalt complexes studied previously.^{21–23}

It has been our goal with the present study to find a system which binds more strongly to cytochrome *c* than the oxochromium(v) complex and shows saturation kinetics, so that the precursor-formation constant and the electron-transfer rate constant could be separated for both the forward and reverse reactions, and this has been achieved with the anionic copper complex of the extended ligand ferrozine (5,6-bis(4-sulfonatophenyl)-3-(2-pyridyl)-1,2,4-triazine). Redox reactions between cytochrome *c* and several cationic copper complexes have been studied before.²⁶ Ferrozine has been widely used for the determination of Co(II), Ru(III), Os(VIII), Au(III), Ag(I) and Cu(I).²⁷ The sulfonic acid group introduces a higher water solubility and makes possible the use of ferrozine for the determination of the iron-binding capacity in plant nutrient solutions and of metals in high purity chemicals. The X-ray structure of the bis(ferrozine)copper complex, which is the subject of this study, has not yet been reported for either the Cu(I) or Cu(II) oxidation states, but is shown schematically in Fig. 1.

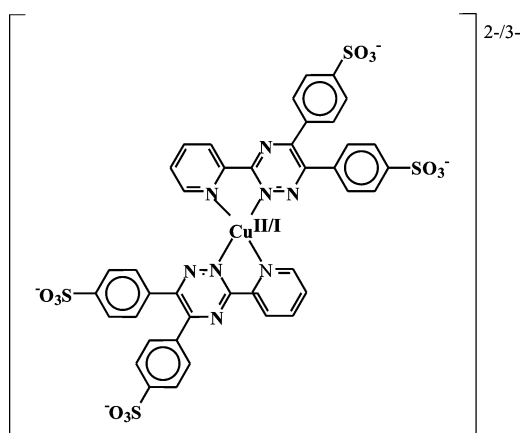


Fig. 1 Bis(ferrozine)copper(II/I) complex.

The preferred geometries of Cu(II) complexes are commonly tetragonally distorted octahedral or square planar, although many trigonal bipyramidal and square pyramidal structures have also been reported; Cu(I) complexes are typically tetrahedrally coordinated. In biologically active metalloproteins and enzymes, the active-site geometry often differs from this. In the blue type I copper proteins plastocyanin and azurin, copper coordinates to two histidine and one cysteine ligand in a trigonal structure. Copper has a further weak axial interaction to methionine. Oxidized and reduced forms of these proteins largely retain this geometry.^{28,29} The CuN₄ center of Cu/Zn bovine superoxide dismutase has a coordination geometry intermediate between square planar and tetrahedral, consisting of three imidazoles and an imidazolate bridging to the Zn(II) center.³⁰ A fifth axial coordination position is occupied by a water molecule.^{31,32} This geometry is retained in both oxidation states of Cu^{III}ZnSOD.³³ Model systems for such copper proteins should therefore retain their coordination geometry during an outer-sphere electron-transfer mechanism. In contrast, simpler copper complexes often tend to adopt different coordination numbers and geometries in different oxidation states. The system reported here demonstrates the importance of these considerations.

Experimental

Reagents

Horse heart cytochrome *c* (type VI, Sigma) was purified and reduced as reported previously.²¹ Concentrations of the cytochrome solutions were determined by UV-Vis spectroscopy.

Double distilled, deionized water was used in the preparation of all solutions. LiNO₃ was used to adjust the ionic strength of the solutions.

Preparation of the Cu(II) complex

For kinetic experiments the Cu(II) complex was prepared *in situ* in TRIS buffer (TRIS = tris(hydroxymethyl)aminomethane, Aldrich) by mixing weighted amounts of CuSO₄·5H₂O and the monosodium salt of the ferrozine ligand (3-(2-pyridyl)-5,6-bis(4-sulfonatophenyl)-1,2,4-triazine, Aldrich), which was generally in 8-fold excess over the copper concentration to ensure complete complex formation. The UV-Vis spectra show only weak absorbance bands at 639 nm ($\epsilon_{\text{max}} = 153 \text{ M}^{-1} \text{ cm}^{-1}$, broad) and 470 nm ($\epsilon = 187 \text{ M}^{-1} \text{ cm}^{-1}$) (Fig. 2). In the absence of TRIS buffer the broad CT band at 639 nm is shifted by 19 nm to higher wavelengths. This points to a medium effect. The pH was kept constant.

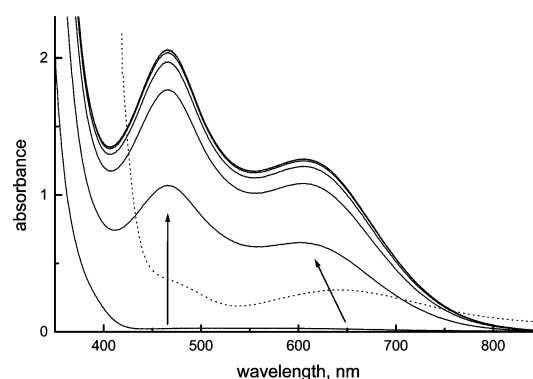


Fig. 2 UV-Vis spectra recorded for the reduction of the Cu(II) complex in N₂-saturated solutions: (· · ·) [Cu(II)] = 2 × 10⁻³ M, pH 7.4, 0.05 M TRIS, I = 0.2 M (LiNO₃), 25 °C, 1 cm path length quartz cell; (—) [Cu(II)] = 1.25 × 10⁻³ M in 0.2 cm path length quartz cell and excess copper powder reacts to the copper(I) complex under the same anaerobic reaction conditions, Δt = 2 h.

Infrared spectra of the crystallized product isolated in the absence of TRIS buffer, synthesized from copper(II) sulfate and a 3-fold excess of the ligand dissolved in less water, showed the following bands [cm⁻¹] (br: broad, m: medium, sp: sharp, s: strong, vs: very strong, w: weak): 3439s, br ν(O–H); 3120m, 3083m ν(C–H_{arom}); 1632m ν(C=N), δ(H–O–H, crystal water), 1613m ν(C=C arom.); 1559w ν(N=N– azo); 1526s ν(C=C arom.); 1403s δ(O–H), 1372s ν(SO₂, sulfonate); 1225vs, 1193vs ν(SO₂, sulfonate); 1120s (sulfate); 1034vs ν(S=O); 805s (1,4-disubstituted benzene); 687m (pyridine); 620vs ν(C–S). Additional bands were observed for the product isolated in the presence of TRIS buffer and ascribed to the coordination of TRIS: 3600sp ν(O–H)_{free}; 3130–3030m ν(NH₃⁺); 2931m br ν_{as}(CH₂), ν(O–H)_{assoc}; 1650–1620m several bands, δ(NH₃⁺); 1475m δ(CH₂); 696m (–CH₂– rocking).

Elemental analysis: crystallized product was isolated in the absence of TRIS buffer in acidic solution (pH about 1) as the fully protonated sulfate salt: [Cu(LH₂)₂]SO₄·3H₂O, CuC₄₀H₃₄N₈O₁₉S₅, calc. (found): C 41.61 (41.17), N 9.71 (9.53), H 2.99 (2.84%); product isolated in the presence of TRIS buffer (L = ligand) (three components A, B, C showed the best result for the elemental analysis and ICP measurement): (A) [Cu(L²⁻)₂(TRIS-NH₃⁺)₄]²⁺SO₄²⁻, (B) [Cu(L + Li)₂(TRIS-NH₃⁺)₂]²⁺SO₄²⁻NO₃⁻, (C) [Cu(L + Na)₂(TRIS-NH₃⁺)₂]²⁺SO₄²⁻NO₃⁻: 0.42 CuC₅₆H₇₂N₁₂O₂₈S₅ (A), 0.48 CuC₄₈H₄₈N₁₁O₂₃S_{4.5}Li₂ (B), 0.1 CuC₄₈H₄₈N₁₁O₂₃S_{4.5}Na₂ (C), calc. (found): C 42.80 (42.16), N 10.75 (10.96), H 3.97 (3.74), S 10.34 (10.34%).

ICP measurements on 9.9 mg of substance isolated in the presence of TRIS buffer dissolved in 15 ml 1% HNO₃ (mean value of three measurements), calc. (found) [mg l⁻¹]: Cu 28.91 (28.93 ± 0.37), Li 3.22 (3.26 ± 0.11), Na 2.18 (1.96 ± 0.62).

EPR-measurements: [Cu(II) complex] = 1×10^{-3} M (without TRIS buffer), water–ethanol (1 : 1), 120 K, ^{63}Cu ($I = 3/2$, 69.2% natural abundance), ^{65}Cu ($I = 3/2$, 30.8% natural abundance). The signal consists of four equally spaced peaks at $g_1 = 2.245$, and of one single line at $g_2 = 2.067$; $A_1(^{63}\text{Cu}, ^{65}\text{Cu}) = 161$ G, $A_2(^{63}\text{Cu}, ^{65}\text{Cu}) = 0$. Using the program Simfonia,³⁵ an axial symmetry simulation fitted the spectrum well with the following parameters: $A = 161$ G, $g_x = g_y = 2.07$, line width = 300 G. For [Cu(II) complex] = 5×10^{-3} M (with TRIS buffer pH 7.4), water–ethanol (1 : 1), 120 K, the signal consists of four equally spaced peaks at $g_1 = 2.222$, and one single line at $g_2 = 2.061$; $A_1(^{63}\text{Cu}, ^{65}\text{Cu}) = 194$ G, $A_2(^{63}\text{Cu}, ^{65}\text{Cu}) = 0$.

Preparation of the Cu(I) complex

The Cu(II) complex was quantitatively reduced to the Cu(I) complex with Cu powder in a synproportionation reaction (Fig. 2). The Cu(I) complex exhibits a strong absorbance band at about 466 nm ($\epsilon_{\text{max}} = 4320 \text{ M}^{-1} \text{ cm}^{-1}$)³⁶ and 609 nm ($\epsilon_{\text{max}} = 2640 \text{ M}^{-1} \text{ cm}^{-1}$). The UV-Vis spectra are similar to those for the established tetrahedral Cu(I) complexes.³⁷ The band at 465 nm is characteristic for a Cu(I) diimine system and is attributed to charge transfer from the filled metal d-orbital to the LUMO of the diimine ligands. Corresponding Cu(II) complexes show broad d–d absorption bands in the range 600–900 nm.³⁸ The two additional nitrogens in the 3-(2-pyridyl)-1,2,4-triazine structure compared to diimine systems have less influence on the position of these bands. Nevertheless, in the absence of TRIS buffer, the band of the Cu(I) complex exhibits a small shift to 458 nm, where also the bis(diimine) compound [Cu(dmphen)₂]⁺ shows a maximum extinction.³⁹ Under aerobic conditions, the characteristic UV-Vis spectrum of Cu(I) disappeared with time. Glassware of the Schlenk type with a 1 cm or 2 mm cuvette directly attached to a reaction reservoir, allowed the reaction of this complex with cytochrome *c* to be followed under strictly anaerobic conditions.

NMR measurements: to avoid oxidation of Cu(I) solutions in D₂O, NMR tubes were sealed with a PTFE plug. The samples prepared in this way were stable for days. The pH was adjusted with diluted NaOD; no correction was made to the pH for the deuterium isotope effect. Samples were deoxygenated by repeated freeze–pump–thaw cycles.

Cu(I) complex without TRIS buffer, 20.8 mM, $I = 0.2$ M (LiNO₃), pH 7.4 (NaOD) in D₂O–TSP (= 3-(trimethylsilyl)propionic acid (sodium salt) as reference).

¹H NMR [δ /ppm, J /Hz; 348 K]: 9.44 (d, br, 1H, pyridine–H3); 8.90 (pseudo-s, 1H, phenyl–H); 8.67, 8.62 (2 pseudo-s, 4H, 2 phenyl–H3,5); 8.35 (d, ³ J (7.8), 1H, pyridine–H6); 8.24 (t, ³ J (7.8), 1H, pyridine–H5); 8.18 (pseudo-s, 1H, phenyl–H); 8.16 (d, ³ J (7.6), 1H, phenyl–H); 8.03 (d, ³ J (7.6), 1H, phenyl–H); 7.86 (t, ³ J (7.6), 1H, pyridine–H4). ⁶³Cu NMR: single peak at 241.5 ppm (40 °C)

In the presence of TRIS buffer, which was in a *ca.* 10-fold excess over Cu(I), no Cu signal could be observed, even if the complex concentration was *ca.* 50 mM and the scan-time at least 6 h. This suggests a labile exchange of buffer and water at the copper centre. The sample temperature could not be lowered far enough to resolve the spectra in aqueous solution.

Measurements

UV-Vis spectra were recorded on either a Hewlett Packard HP8452 or a Shimadzu UV-2101PC spectrophotometer. For extremely high absorbance measurements, a Cary 5G UV-Vis-NIR spectrophotometer was used. IR spectra were recorded in KBr disks on a Mattson Polaris 10410R FT-IR spectrometer. Elemental analysis for Cu, Li and Na were determined on a Spectroflame ICP-AES (Spectro).

A Bruker ESP 300E X-band spectrometer operating at about 9.5 GHz was used for recording EPR spectra. EPR spectrometer settings were as follows (values for solution with TRIS

buffer in parentheses): central field, 3250 G (3000); sweep width, 2500 G (1000); microwave power, 20.1 mW; modulation frequency, 100 kHz; modulation amplitude, 9.434 G; receiver gain, 2.50×10^4 (2.00×10^4); conversion time, 20.48 ms; time constant, 10.24 ms; number of scans, 5; temperature 120 K. The pH of the solutions was measured on a Metrohm 716 DMS Titrino pH-meter. The kinetic traces for the reduction of cytochrome *c* were recorded at 550 and 420 nm where the absorbance was lower. The reactions at ambient pressure were followed using an Applied Photophysics SX-18 MV stopped-flow instrument (Leatherhead, UK), to which an online data acquisition system was connected. The kinetic traces, consisting of 1000 points per trace, were collected, stored and fitted on an Acorn 5000 computer using Applied Photophysics software (Leatherhead, UK). In order to observe the progress of the overall reaction, time-resolved spectra were recorded on an Applied Photophysics SX-18 MV stopped-flow instrument (Leatherhead, UK) equipped with a J&M TIDAS 16–500 diode array detector (Aalen, Germany). A homemade high-pressure stopped-flow system was used for the high pressure kinetic measurements.^{40,41} The kinetic traces consisting of 1000 points per trace, were collected and stored on an IBM-compatible computer using Biologic (Claix, France) software. The rate constants were calculated using the OLIS KINFIT program (Olis, Bogart, Georgia, USA). All instruments were thermostated to ± 0.1 °C. The kinetic traces showed excellent first-order behavior over 5 half-lives. In general, all solutions were prepared under nitrogen to avoid complications with dissolved oxygen. All test solutions were protected from light to avoid photo-induced decomposition. The freshly prepared solutions were transferred into the stopped-flow unit using gastight Optima Graf Fortuna glass syringes (Roth).

Electrochemical measurements were carried out using an EG&G Princeton Applied Research 263 System and the data collected *via* 270/250 Research Electrochemistry Software 4.00. For electrochemical measurements at elevated pressure, a homemade, high-pressure cell similar to that described in the literature⁴² and thermostated to ± 0.1 °C, was employed. Prior to use, the glassy carbon electrode (3 mm diameter) surface was polished with an aqueous suspension of 3 μm alumina followed by 1 μm alumina (Alfa) on a polishing cloth, followed by rinsing with distilled water and further cleaning with a dry tissue. The Pt auxiliary electrode was cleaned in 5 M aqueous HNO₃, rinsed with distilled water and dried with a tissue. The reference electrode consisted of an Ag wire in 0.01 M AgNO₃ and 0.2 M KNO₃ solution. The copper solutions were transferred into the electrochemical cell under nitrogen. Nitrogen was passed through the solution for several minutes to ensure that oxygen was absent. The potassium hexacyanoferrate couple was used as an external standard. Cyclic voltammograms (CV) were scanned beginning in the negative direction from the upper potential limit.

Results and discussion

Structure of bis(ferrozine)–copper complexes in solution

The EPR observations reported here match closely a number of recently reported Cu(II) complexes (hydrotris[3-phenylpyrazolyl-1-yl]borato)(5-phenylpyrazole)bromocopper(II), $g_1 = 2.24$, $g_2 = 2.09$, $A = 167$ G;⁴³ hydrotris[3-phenylpyrazolyl-1-yl]borato)(5-phenylpyrazole)chlorocopper(II), $g_1 = 2.26$, $g_2 = 2.08$, $A = 163$ G;⁴³ (*N,N',N''N'''*-tetra(2-aminoethyl-1,1,2,2-ethanetetraamide))copper(II), $g_1 = 2.012$, $g_2 = 2.049$, $A = 97$ G;⁴⁴ Cu(II) complex of the bleomycin analog 2-[(2-(4-imidazolyl)ethyl)amino]carbonyl]-6-[(2-amino-1,1,2-trimethylpropyl)amino]methyl]pyridine, $g_1 = 2.21$, $g_2 = 2.04$, $A = 165$.⁴⁵ Independent X-ray structures have shown these all to involve a five-coordinate square pyramidal Cu(II) environment. UV-Vis absorption in the region 550–670 nm observed for the Cu(II)–

Table 1 pH-Dependence of the electron transfer reaction between CuL_2^{2-} and cytochrome c^{II} ($[\text{Cu}(\text{II})]=1.75 \times 10^{-4} \text{ M}$, $I=0.1 \text{ M}$, $T=15^\circ \text{C}$, $[\text{cyt } c^{\text{II}}]=1.5 \times 10^{-5} \text{ M}$)

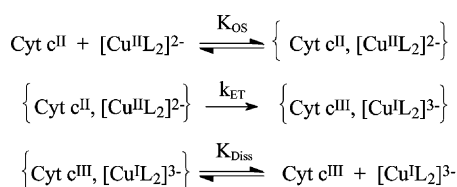
pH	$k_{\text{obs}}/\text{s}^{-1}$
6.6	14.3 ± 0.5
	16.0 ± 0.3
7.0	10.0 ± 0.2
7.2	6.30 ± 0.08
7.4	3.50 ± 0.05
7.7	2.90 ± 0.05
8.0	2.02 ± 0.03
	2.00 ± 0.04
8.4	1.44 ± 0.03
8.8	0.70 ± 0.01

bis(ferrozine) complex is also characteristic of square pyramidal $\text{Cu}(\text{II})$.⁴⁵ In the case of this complex we propose that the labile axial position is occupied by water in aqueous solution with competition from TRIS coordination in the presence of high concentrations of buffer.

Based primarily on the UV-Vis spectra reported above, the $\text{Cu}(\text{I})$ -bis(ferrozine) complex is proposed to be tetrahedral in solution. The electrochemistry is described in more detail below, however, the waveform and observed potentials support a tetrahedral $\text{Cu}(\text{I})$ structure, characterised by a substantially more positive (II/I) reduction potential than that of the square pyramidal $\text{Cu}(\text{II})$ complex from which it is indirectly produced.

Kinetic studies

The oxidation of cytochrome c^{II} was studied under pseudo-first-order conditions, except where it was important to investigate particular trends. The outer-sphere electron transfer mechanism is outlined in Scheme 1. The lowest cytochrome c^{II} concentration was *ca.* 0.015 mM, and the $\text{Cu}(\text{II})$ complex was in more than a 100-fold excess at its maximum concentration. TRIS buffer was selected as reaction medium since it is in many cases accepted to be innocent and, furthermore, exhibits no significant pressure dependence. The pH dependence of the oxidation reaction showed a decrease in rate constant in alkaline solutions (Table 1). For pH higher than *ca.* 8, the fraction of the less reactive alkaline form of cytochrome c increases and slows the overall reaction.



Scheme 1 Outer-sphere mechanism for the oxidation of cytochrome c .

The dependence of the second-order rate constant (Kk_{ET}) on the ionic strength, was measured for the lowest $\text{Cu}(\text{II})$ concentration at pH 7.7, where the rate constant is almost independent of pH. The rate constant decreases with increasing ionic strength as expected for reactants of opposite charge (Fig. 3). At a first glance, the magnitude of rate retardation is surprising since the pseudo-first-order rate constants vary by a factor of 200, which is unusual for reactions between cytochrome c and small molecules. However, the simplified Debye-Hückel equation is only valid if the size of the metal complex can be neglected relative to the cytochrome c redox center. The approaches of van Leeuwen, Koppenol and Rush⁴⁶⁻⁴⁹ predict a much stronger dependence on ionic strength if the reactant radii are similar, as in this case. The contact radius for cytochrome c has been estimated to be 1.66 nm⁵⁰ and for the copper complex *ca.* 1.15 nm.⁵¹

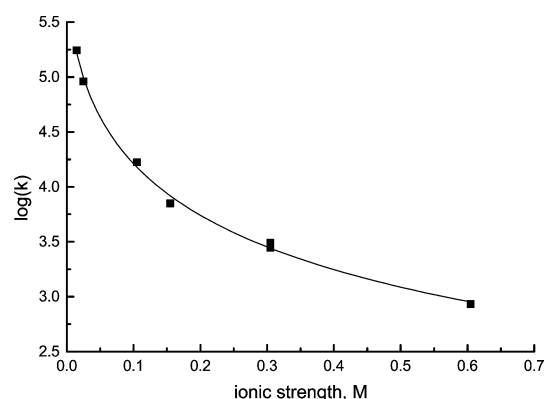


Fig. 3 Ionic strength dependence of the observed rate constant for the oxidation of cytochrome c . Experimental conditions: $[\text{cyt } c^{\text{II}}]=(1.5-1.7) \times 10^{-5} \text{ M}$, $[\text{Cu}(\text{II})]=1.75 \times 10^{-4} \text{ M}$, pH 7.7, 0.05 M TRIS, 15°C , $\lambda=550$ or 420 nm, LiNO_3 used to adjust the ionic strength. Best fit for the equation $y=a+b\lambda^{0.5}/(1+c\lambda^{0.5})$ results in $a=6.18 \pm 0.2$, $b=-9.49 \pm 1.6$ and $c=1.65 \pm 0.4$ for the three parameters.

The $\text{Cu}(\text{II})$ concentration dependence, investigated at an ionic strength of 0.2 M and pH 7.4, clearly shows saturation kinetics (Fig. 4). A Lineweaver-Burk reciprocal plot of eqn. (1), which

$$k_{\text{obs}} = Kk_{\text{ET}}[\text{Cu}^{\text{II}}\text{L}_2^{2-}]/\{1 + K[\text{Cu}^{\text{II}}\text{L}_2^{2-}]\} \quad (1)$$

represents the rate law for the reactions in Scheme 1, results in $K=(7.7 \pm 0.5) \times 10^3 \text{ M}^{-1}$ and $k_{\text{ET}}=6.2 \pm 0.4 \text{ s}^{-1}$ at 288 K.

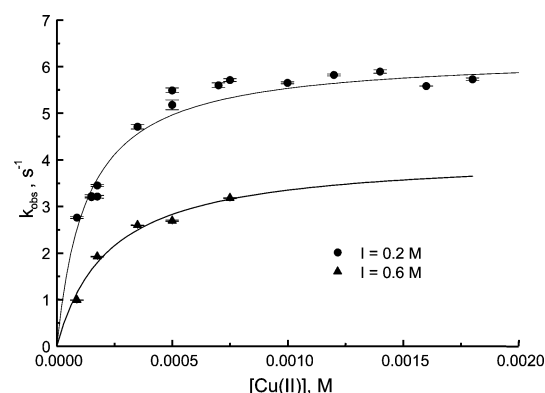


Fig. 4 Plots of k_{obs} vs. the $\text{Cu}(\text{II})$ complex concentration. Experimental conditions: $[\text{cyt } c^{\text{II}}]=(1.5-1.7) \times 10^{-5} \text{ M}$, pH 7.4, 0.05 M TRIS, $I=0.2$ or 0.6 M (LiNO_3), 15°C , $\lambda=550$ and 420 nm. Fit for $I=0.2 \text{ M}$ according to Lineweaver-Burk (—) leads to $k_{\text{ET}}=6.2 \pm 0.4 \text{ s}^{-1}$ and $K=(7.7 \pm 0.5) \times 10^3 \text{ M}^{-1}$. For $I=0.6 \text{ M}$ and low $[\text{Cu}(\text{II})]$ concentrations, k_{ET} and K equal $4.1 \pm 0.3 \text{ s}^{-1}$ and $(4.4 \pm 0.8) \times 10^3 \text{ M}^{-1}$, respectively.

The rate constants were also measured for 0.6 M ionic strength. Due to apparent solubility limitations of the $\text{Cu}(\text{II})$ complex in this medium, only a few reliable experiments could be performed at low $\text{Cu}(\text{II})$ concentrations, and the results are included in Fig. 4. As expected for oppositely charged reactants, the precursor-formation constant decreases with increasing ionic strength.

The temperature dependence of the forward reaction was studied at very low and high $\text{Cu}(\text{II})$ concentrations in order to determine the activation parameters associated with Kk_{ET} and k_{ET} , respectively. Eyring plots for the experimental rate constants are given in Fig. 5. Analysis of the data at low $\text{Cu}(\text{II})$ concentration gives $\Delta H^\ddagger (= \Delta H_{\text{OS}}^\ddagger + \Delta H_{\text{ET}}^\ddagger) = 85 \pm 4 \text{ kJ mol}^{-1}$ and $\Delta S^\ddagger (= \Delta S_{\text{OS}}^\ddagger + \Delta S_{\text{ET}}^\ddagger) = +12 \pm 13 \text{ J K}^{-1} \text{ mol}^{-1}$; from the high $\text{Cu}(\text{II})$ concentration experiments, $\Delta H^\ddagger (= \Delta H_{\text{ET}}^\ddagger) = 89 \pm 4 \text{ kJ mol}^{-1}$ and $\Delta S^\ddagger (= \Delta S_{\text{ET}}^\ddagger) = -79 \pm 15 \text{ J K}^{-1} \text{ mol}^{-1}$. From these, the reactant pre-association contributions can be resolved: $\Delta H_{\text{OS}}^\ddagger = -4 \pm 8 \text{ kJ mol}^{-1}$ and $\Delta S_{\text{OS}}^\ddagger = 91 \pm 28 \text{ J K}^{-1} \text{ mol}^{-1}$.

Outer-sphere electron transfer reactions between similarly charged, octahedral metal complexes have significantly negative

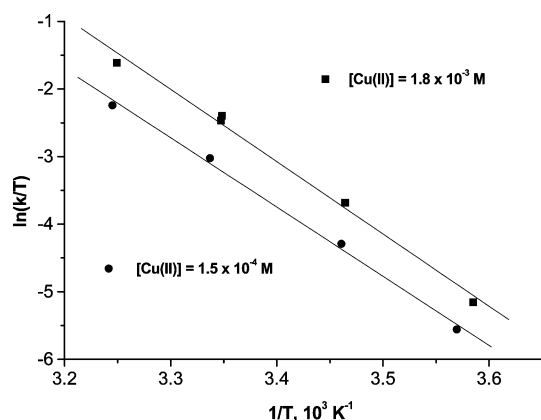


Fig. 5 Eyring plots for the oxidation of cytochrome *c*. Experimental conditions: [cyt c^{II}] = $(1.5\text{--}1.7) \times 10^{-5}$ M, pH 7.4, 0.05 M TRIS, $I=0.2$ M (LiNO_3), $\lambda=550$ or 420 nm. [Cu(II)] = 1.5×10^{-4} M, $\Delta H^\ddagger=85 \pm 4$ kJ mol $^{-1}$, $\Delta S^\ddagger=-61 \pm 13$ J K $^{-1}$ mol $^{-1}$, ΔG^\ddagger (288 K) = 68 kJ mol $^{-1}$; [Cu(II)] = 1.8×10^{-3} M, $\Delta H^\ddagger=89 \pm 4$ kJ mol $^{-1}$, $\Delta S^\ddagger=-79 \pm 15$ J K $^{-1}$ mol $^{-1}$, ΔG^\ddagger (288 K) = 66 kJ mol $^{-1}$.

activation entropies in the range from -100 to -150 J K $^{-1}$ mol $^{-1}$ due to increased electrostriction in the precursor complex.⁵² Redox reactions between a metal complex and a metalloprotein generally have more positive values, typically between -5 and 10 J K $^{-1}$ mol $^{-1}$. In the formation of the precursor complex, the reorganisation of the solvent molecules at the protein occurs only to a small extent.⁵² While the changes in electrostriction which accompany simple ion association can be predicted in a qualitative sense, the effects accompanying association of reactants on a protein surface are much more open to conjecture. Charges are typically dispersed over the surface; local hydrophobic and hydrophilic phenomena may come into play. In the system studied here, both the cytochrome and the Cu-bis(ferrozine) complex have localized ionic charges over their surfaces. The energy components arising from the pre-association and from the electron transfer stages however can be resolved. The small value of ΔH_{OS} is consistent with a non-specific interaction. The outer-sphere process is driven by entropy generated in the cytochrome/complex preassociation. The activation parameters of the electron transfer step within the outer-sphere complex indicate a significant enthalpic requirement and an entropy change which suggests a structurally constrained process.

Taking particular care to avoid any contact with air, the reverse reaction between the Cu(I) complex and cytochrome c^{III} was studied at an ionic strength of 0.2 M and pH 7.4 by UV-Vis spectroscopy. Fig. 6 shows the formation of the characteristic α -band at 550 nm and the shift of the γ -soret band to 420 nm for cytochrome c^{II} . As with the forward reaction, the kinetic

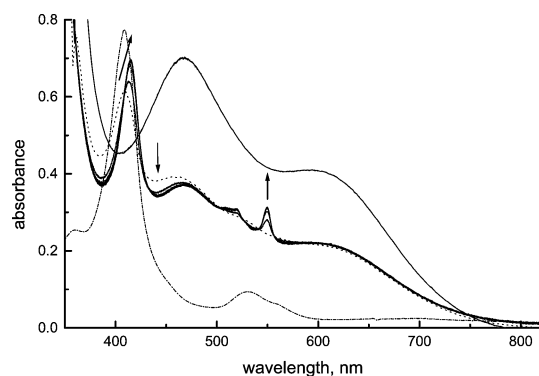


Fig. 6 UV-Vis spectra of the reactants for the reduction of cytochrome *c* in N_2 saturated solutions: (---) [cyt c^{III}] = ca. 4×10^{-5} M, (—) [Cu(I)] = 8×10^{-4} M, pH 7.4, 0.05 M TRIS, $I=0.2$ M (LiNO_3), 15 °C, 0.2 cm cuvette; (···) calculated curve for the reactants in 0.2 cm cuvette before mixing under anaerobic reaction condition; overall reaction time about 40 min.

data showed a rate saturation at higher Cu(I) concentrations and the data were fitted to an analogous expression to eqn. (1). The resulting values are $K' = (2.0 \pm 0.2) \times 10^3$ M $^{-1}$ and $k'_{\text{ET}} = 0.014 \pm 0.001$ s $^{-1}$ at 288 K (Fig. 7). These data can be combined with those from the forward reaction to produce a free energy profile for the overall reaction (Fig. 8).

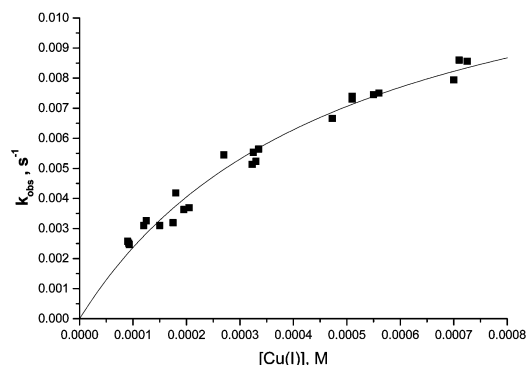


Fig. 7 Plot of k_{obs} vs. concentration of the Cu(I) complex. Experimental conditions: [cyt c^{III}] = 1.7×10^{-5} M, pH 7.4, 0.05 M TRIS, $I=0.2$ M (LiNO_3), 15 °C, $\lambda=550$ nm. Fit according to eqn. (1) results in $k_{\text{ET}}=0.014 \pm 0.001$ s $^{-1}$ and $K=(2.0 \pm 0.2) \times 10^3$ M $^{-1}$

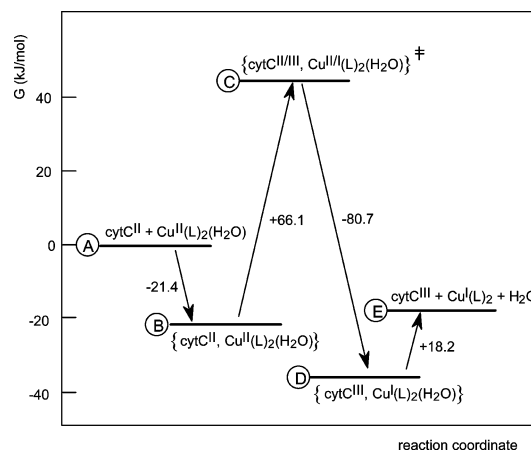


Fig. 8 Free energy profile for the overall reaction measured with respect to free energy of the reactants.

Stopped-flow experiments on the forward reaction at the lowest and highest Cu(II) concentrations at 288 K and 0.2 M ionic strength were carried out at elevated pressures. The plots of $\ln(k_{\text{obs}})$ vs. pressure are shown in Fig. 9, from which $\Delta V^\ddagger = +8.8 \pm 0.6$ and $+8.0 \pm 0.7$ cm 3 mol $^{-1}$ for the low and high Cu(II) concentrations, respectively. The pre-association and electron transfer components for the forward reaction can therefore be

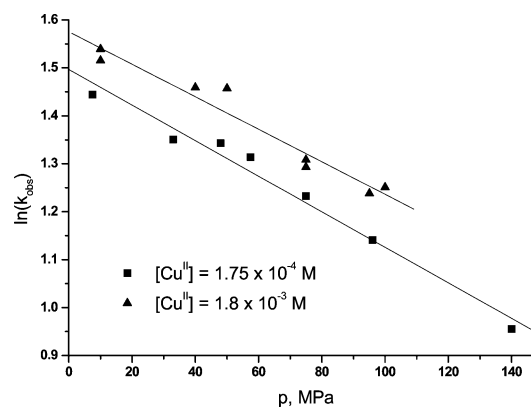


Fig. 9 Effect of pressure on k_{obs} . Experimental conditions: [cyt c^{III}] = $(1.5\text{--}1.7) \times 10^{-5}$ M, pH 7.4, 0.05 M TRIS, $I=0.2$ M (LiNO_3), $\lambda=550$ nm. For [Cu(II)] = 1.75×10^{-4} and 1.8×10^{-3} M, the calculated activation volumes are $+8.8 \pm 0.6$ and $+8.0 \pm 0.7$ cm 3 mol $^{-1}$, respectively.

resolved to give $\Delta V_{\text{OS}} = +0.8 \pm 1.3$ and $\Delta V_{\text{ET}}^{\ddagger} = +8.0 \pm 0.7$ $\text{cm}^3 \text{mol}^{-1}$. ΔV_{OS} is small, as expected on the basis of other measurements and calculated estimates of outer-sphere metal complex preassociations.^{53,54}

In order to place the transition state on a complete volume profile for the reaction, a measure of the overall reaction volume, ΔV , is required. The contribution from the cytochrome *c*^{III/II} couple to this has been shown to be $+5 \text{ cm}^3 \text{mol}^{-1}$.²⁴ Volume changes associated with the Cu(II)/Cu(I) reduction are expected to have both electrostrictive and intrinsic contributions. On the basis of the change in formal charge of the Cu complexes (2- to 3-) and using the observations that ΔV is typically around $4 \text{ cm}^3 \text{mol}^{-1}$ per unit of Δz^2 for many complexes⁵⁴⁻⁵⁷ this would contribute $-20 \text{ cm}^3 \text{mol}^{-1}$. However, evidence is increasing that electrostrictive volume changes seem to be very localized around the redox center.⁵⁷⁻⁵⁹ As is clear from Fig. 1, the sulfonate groups are on the perimeter of the complexes. So on this basis, we propose that it is the 2+/1+ change on the Cu center that will determine the electrostrictive change, leading to a contribution to ΔV of around $+12 \text{ cm}^3 \text{mol}^{-1}$. Turning to intrinsic contributions, in comparable Cu^{II}N₄ systems, the Cu-N bond increases by only *ca.* 0.1 Å during the reduction to the Cu(I) complex³⁷ but the water ligand in the square pyramidal Cu(II) complex is lost to bulk solvent when the coordination changes to tetrahedral Cu(I). Although there are no directly comparable data available, the estimation of the change in volume for the full addition or loss of a solvent ligand is at the centre of the interpretation of data for solvent exchange processes.⁶⁰ Swaddle⁶¹ developed the generally accepted value for the volume change for limiting octahedral A or D mechanisms as $-13.5 \text{ cm}^3 \text{mol}^{-1}$ or $+13.5 \text{ cm}^3 \text{mol}^{-1}$, respectively. The water exchange on tetrahedral $\text{Be}(\text{H}_2\text{O})_4^{2+}$ is the most associative of such aqua-exchanges⁶² and, at $-13.5 \text{ cm}^3 \text{mol}^{-1}$, approaches the 'theoretical' limit of a limiting A process. The difference in partial molar volumes for eight- and nine-coordinate aqualanthanide ions is similarly around $13 \text{ cm}^3 \text{mol}^{-1}$.⁶³ We therefore estimate the total volume change for the reaction of cytochrome *c* with $\text{Cu}(\text{L})_2(\text{H}_2\text{O})^{2+}$ to be $+5 + 12 + 13 = +30 \text{ cm}^3 \text{mol}^{-1}$. In the absence of the loss of a water molecule, the overall reaction volume would only be $+17 \text{ cm}^3 \text{mol}^{-1}$.

These activation and reaction volume data are brought together in Fig. 10. The indication is that the transition state lies early in the overall volume change for the reaction. This should be compared with the redox reactions of cytochrome *c*^{III/II} with octahedral Ru(III)/Ru(II) complexes,^{21,23} where the transition state is at a point very close to 50% of the total volume change. These cases, however, do not involve a change in coordination of the metal centre. We therefore suggest that in the system reported here, the transition state occurs at a point where the

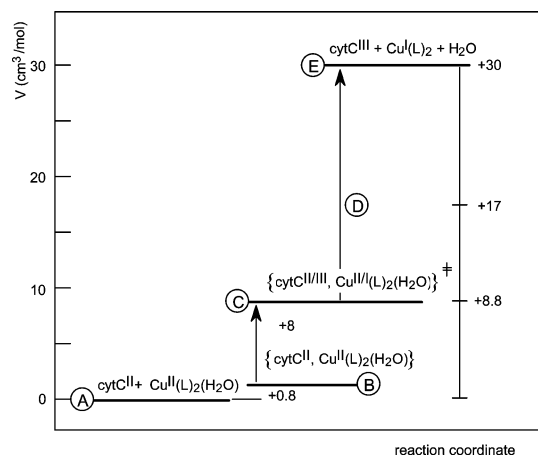


Fig. 10 Volume profile for the oxidation of cytochrome *c* by the Cu(II) complex, measured with respect to the molar volume of reactants.

electron is symmetrically poised within the interaction of the cytochrome *c* with the five-coordinate Cu(II)/(I) species and that the intrinsic volume change due to water loss occurs subsequent to this step.

This is the first report of a cytochrome *c* redox system where the pre-association step and kinetics of electron transfer within the outer-sphere complex have been resolved for both the forward and reverse reactions. The results lead to free energy and volume profiles for the process from which some important mechanistic conclusions can be drawn.

Electrochemical studies

Electrochemical methods were also used to investigate the redox behavior of the Cu(II)-bis(ferrozine) system; it was hoped that carrying out such measurements as a function of high pressure might provide an independent estimate of the reaction volume of the Cu(II/I) couple, which when combined with the known redox volume for cytochrome *c* could be used to establish the overall reaction volume. A CV typical of those observed for the bis(ferrozine)-Cu^{III} system at ambient and elevated pressures is shown in Fig. 11. We have proposed above that the Cu(II) and Cu(I) complexes differ in their coordination geometry and this is reflected in the CV experiment. The geometry of the complex and the coordination number seem to affect the potential more than the nature of the ligand system, with tetrahedral complexes showing the more positive potentials. Among examples of particular relevance to the system studied here are Cu^{III}(TET) (TET = 2,2'-bis(6-(2,2'-bipyridyl))biphenyl), approximately tetrahedral geometry, $E = 0.72 \text{ V}$ (NHE ref.)³⁷ = 0.04 V (Ag/0.01 M Ag⁺ ref.); bis(2,9-dimethyl-1,10-phenanthroline)copper(II/I), tetrahedral, 0.594 V (NHE),⁶⁴ -0.09 V (Ag/Ag⁺); bis(2,9-dimethyl-4,7-bis(sulfonatophenyl)-1,10-phenanthroline)copper(II/I), tetrahedral, 0.62 V (NHE),⁵¹ -0.06 V (Ag/Ag⁺); square pyramidal $[\text{Cu}^{\text{III}}(\text{Him})_2\text{DAP}]^{2+}$ and $[\text{Cu}^{\text{III}}(\text{py})_2\text{DAP}]^{2+}$ (DAP = 2,6-bis[1-((2-imidazol-4-pyridin-2-yl)ethyl)imino]ethyl]pyridine), -0.27 and -0.14 V (SCE ref.) in acetonitrile,⁶⁵ -0.71 V and -0.58 V (Ag/Ag⁺).

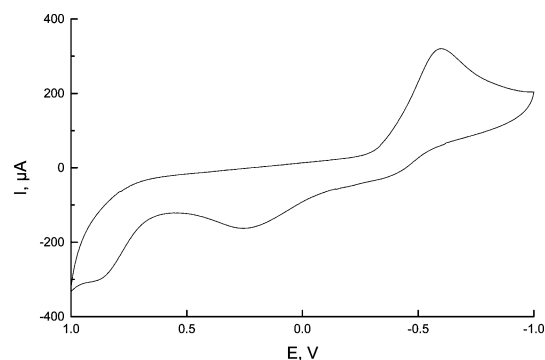
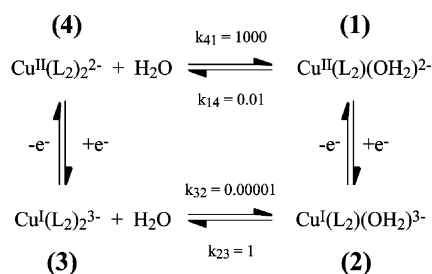


Fig. 11 Typical cyclic voltammogram recorded for the Cu^{III}L₂ redox system. Experimental conditions: $[\text{Cu}(\text{II})] = 1.8 \times 10^{-3} \text{ M}$, pH 7.4, 0.05 M TRIS, $I = 0.2 \text{ M}$ (NaClO₄), pressure = 70 MPa, scan rate 100 mV s^{-1} . The second CV cycle is shown.

A series of simulations were carried out using the electrochemical simulation program ESP⁶⁶ operating within an EC⁶⁷ mechanism represented in Scheme 2. Similar simulations have been performed for other copper complexes in the past.^{68,69} The key parameters which affect the form of the CV wave are the reduction potentials of species (1) and (4) and the rate constants k_{41} , k_{14} , k_{23} and k_{32} . ESP can in principle be used to calculate the parameters controlling the electrochemistry and our aim was to use this to resolve the couples which contribute to the overall process. However, it was found that many parameters were coupled to such extent that uncertainties were large or convergence was not obtained. The analysis reported here, while qualitatively very useful in understanding the nature of the chemistry operating, could not be used to resolve the



Scheme 2 Reaction scheme based on an EC mechanism.

high-pressure electrochemistry data as we had hoped. In order to reproduce the general features of the experimental CV however, the key characteristics of the model were that the reduction potential for the five-coordinate system, (1) to (2), must be more negative than the potential for the reduction of the tetrahedral species, (4) to (3), and that rate constants, and the equilibrium constants determined by their ratios, for the non redox interconversions must be such that a labile Cu(II) species (4) favors the aquated form (1) and a less labile Cu(I) species (2) favors the uncoordinated complex (3).

During the negative sweep, reduction of the square pyramidal Cu(II)L₂(H₂O) favored in solution leads to formation of the peak with a maximum around -0.7 V (Ag/Ag⁺). At the sweep rates used, our experiments suggest substantial, but not complete conversion to the uncoordinated tetrahedral species (3), which is then oxidized on the return sweep to generate the peak observed around +0.3 V to produce first the four-coordinate Cu(II) species (4), which rapidly aquates to produce the original and most stable Cu(II) product (1). The consequence is that no reduction peak of (4), complementary to the oxidation of (3) is observed. We have set the rate constant for water loss from the five-coordinate Cu(I) species produced, k_{23} , at around 1 s⁻¹. We have assumed a rate constant for aquation of (4) of 1000 s⁻¹; higher values, which are probably reasonable for a Cu(II) species, make the simulation very slow and have no measurable effect on the waveform. The key characteristics are that k_{23}^{-1} is comparable with the timescale of the experiment, whereas k_{41}^{-1} is fast on the timescale of the experiment. Combined with the estimates of relative stability of the four- and five-coordinate forms of the Cu(II) and Cu(I) complexes outlined below, we set $k_{32} = 1 \times 10^{-5} \text{ s}^{-1}$ and $k_{14} = 1 \times 10^{-2} \text{ s}^{-1}$ for the CV simulation shown in Fig. 12. A pictorial representation of these species and processes is given in Scheme 3.

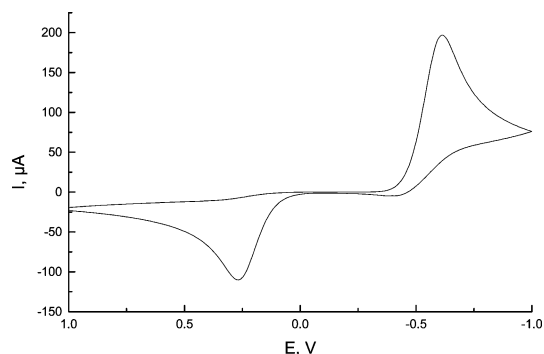
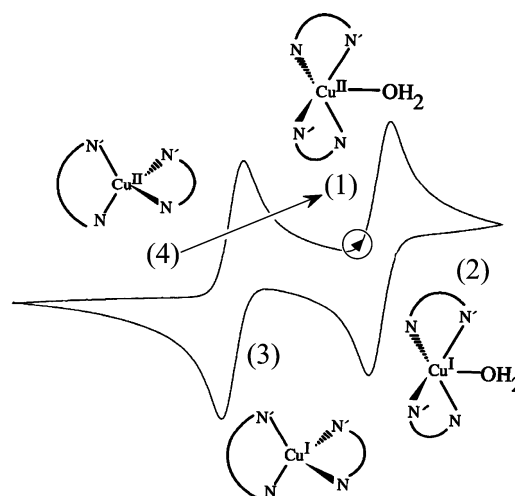


Fig. 12 CV simulation using the program ESP. Parameters were $E_{12} = -0.5 \text{ V}$, $E_{43} = +0.1 \text{ V}$, $k_{23} = 1 \text{ s}^{-1}$, $k_{32} = 0.00001 \text{ s}^{-1}$, $k_{41} = 1000 \text{ s}^{-1}$, $k_{14} = 0.01 \text{ s}^{-1}$.

From the free energy profile derived from our solution kinetic data (Fig. 8) the overall redox reaction has a driving force of -17.8 kJ mol⁻¹ or 0.184 V. Drawing on the known reduction potential of cytochrome *c* of +0.260 V vs. NHE²³ (-25.1 kJ mol⁻¹), this leads to a predicted energy change for the isolated reduction of (1) to (3) of -42.9 kJ mol⁻¹ (+0.445 V vs. NHE).



Scheme 3 Summary of the formation and conversion of species during a cyclic voltammetric scan, based on an EC mechanism.

Though not accurate enough for our other quantitative purposes, fitting the experimental waveform using ESP produced quite reproducible values for the best fit reduction potentials of close to -0.50 V for the five-coordinate Cu(II) complex (1) and close to +0.10 V for the four-coordinate Cu(II) complex (4), each with respect to our Ag/Ag⁺(0.01 M) reference electrode. These then give +0.78 V (vs. NHE) for E_{43} and +0.18 V for E_{12} , corresponding to -75.3 kJ mol⁻¹ for ΔG_{43} and -17.4 kJ mol⁻¹ for ΔG_{12} . These reduction potentials would indicate that while the five-coordinate Cu(II) complex ($E = +0.78 \text{ V}$) is clearly capable of oxidizing cytochrome *c* (+0.26 V), the four-coordinate Cu(II) complex (+0.18 V) is not.

Referring to Scheme 2, it is an obvious requirement that the free energy change ΔG_{13} should be independent of the pathway (1, 2, 3) or (1, 4, 3), that is: $\Delta G_{12} + \Delta G_{23} = \Delta G_{14} + \Delta G_{43}$. It then follows that $\Delta G_{23} + \Delta G_{41} = -57.9 \text{ kJ mol}^{-1}$, or $K_{23}K_{41} = 3 \times 10^{10}$. Arbitrarily, but consistent with the requirements of the simulation that both K_{23} and K_{41} appear to lie heavily to the product side, we could simply assign $\Delta G_{23} = \Delta G_{41} = -29.0 \text{ kJ mol}^{-1}$. Based on this approach, $\Delta G_{143} = 29.0 - 75.3 = -46.3 \text{ kJ mol}^{-1}$ and $\Delta G_{123} = -17.3 - 29.0 = -46.3 \text{ kJ mol}^{-1}$, both in agreement with -42.9 kJ mol⁻¹ obtained from the solution kinetics. Alternatively, working from the kinetically determined value of ΔG_{13} of -42.9 kJ mol⁻¹, we could use the electrochemical potentials to calculate ΔG_{41} as -32.4 kJ mol⁻¹ and ΔG_{23} as -25.6 kJ mol⁻¹.

Conclusions

This redox reaction of cytochrome *c* is controlled by an overall combination of the effective formation of an ion-pair precursor complex and the reorganization of the coordination sphere of the copper complex closely connected with the electron transfer step. The forward reaction is characterized by a significant volume increase during the reduction of Cu(II), which can be ascribed to a decrease in electrostriction during the redox process and the subsequent release of a solvent molecule from the Cu(I) coordination sphere. The transition state of the redox process is located approximately halfway between the reactant and product states on a volume basis, which means that necessary reorganization of the reactants prior to the electron transfer is very similar for the process in both directions. The implication is that the complementary reaction of oxidized cytochrome *c* with the Cu(I) complex requires aquation and expansion of the Cu(I) coordination sphere immediately prior to the reorganisational activation in the electron transfer step. Symmetrical volume profiles have also been reported for the reactions of cytochrome *c* with a series of pentammine-ruthenium complexes.²³ However, in those cases the precursor-

formation step could not be separated kinetically from the electron transfer step, *i.e.* the volume profile represented the combined kinetic and thermodynamic parameters for the overall electron transfer process, and the ruthenium complexes did not involve a change in coordination as a result of the redox reaction. In the present study, such a separation has been accomplished and the constructed free energy and volume profiles clearly reflect this. The symmetric nature of the volume profile for the redox process demonstrates that reorganization of the reactants follow a similar pattern for all these systems in both the forward and reverse reactions. Furthermore, the fact that $\Delta V^\ddagger \approx \Delta V/2$ for the electron transfer step implies in terms of the Marcus cross relationship that the volumes of activation for the self-exchange reactions on cytochrome *c* and the copper complex must be approximately equal and opposite in sign. Unfortunately, such data is presently not available but would add a further dimension to this work.

Acknowledgements

The authors gratefully acknowledge financial support from the Deutsche Forschungsgemeinschaft through the Graduiertenkolleg "Homogeneous and Heterogeneous Electron Transfer".

References

- 1 R. Huber, *Angew. Chem.*, 1989, **7**, 849.
- 2 B. N. Hoffman, M. J. Natan, J. M. Nocek and S. A. Wallin, *Struct. Bonding (Berlin)*, 1991, **75**, 86.
- 3 M. J. Therien, J. Chang, A. L. Raphael, B. E. Bowler and H. B. Gray, *Struct. Bonding (Berlin)*, 1991, **75**, 110.
- 4 D. N. Beratan, J. M. Onuchic and H. B. Gray, *Met. Ions Biol. Syst.*, 1992, **27**, 97.
- 5 N. M. Kostic, *Met. Ions Biol. Syst.*, 1991, **27**, 129.
- 6 J. R. Winkler and H. B. Gray, *Chem. Rev.*, 1992, **92**, 369.
- 7 G. McLendon and R. Hake, *Chem. Rev.*, 1992, **92**, 481.
- 8 V. L. Davidson, *Biochemistry*, 1996, **35**, 14035.
- 9 P. X. Qi, D. L. Di Stefano and A. J. Wand, *Biochemistry*, 1994, **33**, 6408.
- 10 G. R. Moore and G. W. Pettigrew, *Cytochromes c: Evolutionary, Structural and Physicochemical Aspects*, Springer-Verlag, Berlin, 1990.
- 11 J. S. Zhou and N. M. Kostic, *Biochemistry*, 1993, **32**, 4539.
- 12 T. Hayashi, Y. Gitomi and H. Ogoshi, *J. Am. Chem. Soc.*, 1998, **120**, 4910.
- 13 J. Lahiri, G. D. Fate, S. B. Ungashe and J. T. Groves, *J. Am. Chem. Soc.*, 1996, **118**, 2347.
- 14 J. S. Zhou, E. S. V. Granada, N. B. Leontis and M. A. J. Rodgers, *J. Am. Chem. Soc.*, 1990, **112**, 5074.
- 15 K. K. Clark-Ferris and J. Fisher, *J. Am. Chem. Soc.*, 1985, **107**, 5007.
- 16 G. D. Armstrong, J. A. Chambers and A. G. Sykes, *J. Chem. Soc., Dalton Trans.*, 1986, 755.
- 17 J. Butler, D. M. Davies and A. G. Sykes, *J. Am. Chem. Soc.*, 1981, **103**, 469.
- 18 J. Butler, S. K. Chapman, D. M. Davies, A. G. Sykes, S. H. Speck, N. Osheroff and E. Margoliash, *J. Biol. Chem.*, 1983, **258**, 6400.
- 19 J. S. Zhou and N. M. Kostic, *J. Am. Chem. Soc.*, 1991, **113**, 7040.
- 20 Y. Patterson, S. W. Englander and H. Roder, *Protein Sci.*, 1990, 755.
- 21 B. Bänsch, M. Meier, P. Martinez, R. van Eldik, C. Su, J. Sun, S. S. Isied and J. F. Wishart, *Inorg. Chem.*, 1994, **33**, 4744.
- 22 M. Meier and R. van Eldik, *Chem. Eur. J.*, 1997, **3**, 39.
- 23 M. Meier, J. Sun, J. F. Wishart and R. van Eldik, *Inorg. Chem.*, 1996, **35**, 1564.
- 24 J. Sun, J. F. Wishart, R. van Eldik, R. D. Shalders and T. W. Swaddle, *J. Am. Chem. Soc.*, 1995, **117**, 2600.
- 25 M. Körner and R. van Eldik, *Eur. J. Inorg. Chem.*, 1999, 1805.
- 26 M. A. Augustin and J. K. Yandell, *Inorg. Chem.*, 1979, **18**, 577.
- 27 G. Ai-Jabari and B. Jaselskis, *Talanta*, 1987, **34**, 479.
- 28 W. E. B. Shepard, B. F. Anderson, D. A. Lewandoski, G. E. Norris and E. N. Baker, *J. Am. Chem. Soc.*, 1990, **112**, 7817.
- 29 J. M. Guss, P. R. Harrowell, M. Murata, V. A. Norris and H. C. Freeman, *J. Mol. Biol.*, 1986, **192**, 361.
- 30 J. A. Tainer, E. D. Getzoff, K. M. Beem, J. S. Richardson and D. C. Richardson, *J. Mol. Biol.*, 1982, **160**, 181.
- 31 J. A. Fee and G. B. Gaber, *J. Biol. Chem.*, 1972, **247**, 60.
- 32 N. Boden, M. C. Holmes and P. F. Knowles, *Biochem. J.*, 1979, **177**, 303.
- 33 W. R. Rypniewski, S. Mangani, B. Bruni, P. L. Orioli, M. Casati and K. S. Wilson, *J. Mol. Biol.*, 1995, **251**, 282.
- 34 Solutions were prepared under the same conditions and same concentrations as for the high-pressure stopped-flow and electrochemistry measurements. After 2 d the precipitated green powder was filtered off, washed with diethyl ether, and dried for 3 h. The coordination of the TRIS buffer to Cu(II) can occur *via* the alcohol group.
- 35 P. Printz and R. Weber, SimFonia, Version 1.2, Bruker, 1992.
- 36 M. A. Ditzler, H. Pierre-Jacques and S. A. Harrington, *Anal. Chem.*, 1986, **58**, 195; S. K. Kundra, M. Katyal and R. P. Singh, *Anal. Chem.*, 1974, **46**, 1605.
- 37 E. Müller, C. Piguet, G. Bernardelli and A. F. Williams, *Inorg. Chem.*, 1988, **27**, 849.
- 38 B. Hathaway, *Struct. Bonding (Berlin)*, 1984, **57**, 55.
- 39 H. Doine, Y. Yano and T. W. Swaddle, *Inorg. Chem.*, 1989, **28**, 2319.
- 40 R. van Eldik, D. A. Palmer, R. Schmidt and H. Kelm, *Inorg. Chim. Acta*, 1981, **50**, 131.
- 41 R. van Eldik, W. Gaede, S. Wieland, J. Kraft, M. Spitzer and D. A. Palmer, *Rev. Sci. Instrum.*, 1993, **64**, 1355.
- 42 H. Doine, T. W. Whitcombe and T. W. Swaddle, *Can. J. Chem.*, 1992, **70**, 81.
- 43 M. A. Halcrow, J. E. Davies and P. R. Raithby, *Polyhedron*, 1997, **16**, 1535.
- 44 Z. Shourong, L. Qinhuai, S. Menchang and D. Anbang, *Polyhedron*, 1992, **11**, 941.
- 45 H. Kurosaki, K. Hayashi, Y. Ishikawa, M. Goto, K. Anada, I. Taniguchi, M. Shionoya and E. Kimura, *Inorg. Chem.*, 1999, **38**, 2824.
- 46 W. H. Koppenol, *Biophys. J.*, 1980, **29**, 493.
- 47 J. W. van Leeuwen, F. Mofers and E. Veerman, *Biochim. Biophys. Acta*, 1981, **635**, 434.
- 48 J. W. van Leeuwen, *Biochim. Biophys. Acta*, 1983, **743**, 408.
- 49 J. D. Rush, J. Lan and W. H. Koppenol, *J. Am. Chem. Soc.*, 1987, **109**, 2679.
- 50 K. Heremans, M. Bormans, J. Snauwaert and H. Vandersypen, *Faraday Discuss. Chem. Soc.*, 1982, **74**, 343.
- 51 A. E. Allan, A. G. Lappin and M. C. M. Laranjeira, *Inorg. Chem.*, 1984, **23**, 477.
- 52 N. Sutin, *Adv. Chem. Ser.*, 1977, **162**, 156.
- 53 I. Krack and R. van Eldik, *Inorg. Chem.*, 1990, **29**, 1700.
- 54 Y. Fu and T. W. Swaddle, *Inorg. Chem.*, 1999, **38**, 876.
- 55 J. I. Sachanidis, R. D. Shalders and P. A. Tregloan, *Inorg. Chem.*, 1994, **33**, 6180.
- 56 J. I. Sachanidis, R. D. Shalders and P. A. Tregloan, *Inorg. Chem.*, 1996, **35**, 2497.
- 57 T. W. Swaddle and P. A. Tregloan, *Coord. Chem. Rev.*, 1999, **187**, 255.
- 58 B. D. Yeomans, L. S. Kelso, P. A. Tregloan and F. R. Keene, *Eur. J. Inorg. Chem.*, 2001, 23.
- 59 H. C. Bajaj, P. A. Tregloan and R. van Eldik, in preparation.
- 60 T. Kowall, P. Caravan, H. Bourgeois, L. Helm, F. P. Rotzinger and A. E. Merbach, *J. Am. Chem. Soc.*, 1998, **120**, 6569.
- 61 T. W. Swaddle, *Inorg. Chem.*, 1983, **22**, 2665.
- 62 P. A. Pittet, G. Elbaze, L. Helm and A. E. Merbach, *Inorg. Chem.*, 1990, **29**, 1936.
- 63 T. W. Swaddle and M. K. S. Mak, *Can. J. Chem.*, 1983, **61**, 473.
- 64 N. Al-Shatti, A. G. Lappin and A. G. Sykes, *Inorg. Chem.*, 1981, **20**, 1466.
- 65 J. A. Goodwin, D. M. Stanbury, L. J. Wilson, C. W. Eigenbrot and W. R. J. Scheidt, *J. Am. Chem. Soc.*, 1987, **109**, 2979.
- 66 C. Nervi (http://chpc06.ch.unito.it/esp_manual.html) Electrochemical Simulations Package, ESP 2.4, 1998.
- 67 EC-Notation: E: 1-e⁻ transfer at the electrode, C: homogeneous chemical reaction coupled to the electrode reaction.
- 68 M. M. Bernardo, P. V. Robandt, R. R. Schroeder and D. B. Rorabacher, *J. Am. Chem. Soc.*, 1989, **111**, 1224.
- 69 N. E. Meagher, K. L. Juntunen, C. A. Salhi, L. A. Ochrymowycz and D. B. Rorabacher, *J. Am. Chem. Soc.*, 1992, **114**, 10411.